Development of Dragline Excavation Model for Operation Planning

Haoquan Liu, Michael Kearney, Kevin Austin
The University of Queensland, Australia
h.liu@uq.edu.au, m.kearney@uq.edu.au, kevin.austin@uq.edu.au

Abstract

Draglines are gigantic excavators commonly used to remove overburden that sits above a target mineral reserve in surface mining. Their operational efficiency is greatly affected by the sequence of positions where the dragline operates and the removal and disposal of material at each position. In this paper, we develop two dragline excavation models that can be used for planning and optimizing dragline operations. The first of these models is developed using mixed-integer linear programming (MILP) while the second model is developed using a geometric approach. These models are developed for different applications in dragline operation planning. Comparison is made between these models and their advantages and limitations are identified.

1 Introduction

Draglines are one of the largest machines used in surface mining (see Figure 1). Each dragline is a self-contained excavation system that is able to remove and dispose of the overburden without the assistance of other mining machines. In surface mining, draglines are employed in excavating a long strip of overburden sitting above the target mineral reserve. Figure 2 shows the typical geometric structure of a surface coal mine without the dragline. A strip of overburden is removed and dumped to the immediately adjacent strip where the coal has already been extracted. A large pile of material is formed by the dumped material and extended on the adjacent strip, which is called the spoil pile. The excavation of a strip of overburden is scheduled in a sequence of blocks along the strip. Each of the blocks contains a certain amount of overburden and is defined by the strip width, the block length, the overburden depth and the angle of the working surface. A block of overburden is removed while the dragline moves through a sequence of positions (positioning). At each position, the dragline performs cyclic operations of digging the material from the block and dumping it onto the spoil pile. Specifically, each dig-dump cycle comprises: filling the bucket by dragging it with the drag rope towards the fairlead; hoisting the loaded bucket with the hoist rope while swinging it to the spoil pile; dumping the material; and swinging and lowering the bucket back to the block to start the next cycle. The drag rope and the hoist rope are controlled by separate motors that are located inside the machinery house. A dragline repeats this dig-dump cycle a thousand times a day on average with a cycle time of around one minute [Humphrey and Wagner, 2011; Mirabediny, 1998].

Currently the dragline operations, including digging, dumping and positioning, are planned and executed by the operators. This results in inconsistent excavation performance between operators with different levels of experience and further decreases overall productivity. The benefits of enhancing the excavation productivity are indicated by analysis from 2006 that estimates that a 1% improvement in dragline productivity is valued at around AUD $1M per machine per year [Corke *et al.*, 2006]. Following an optimized excavation plan helps achieve consistent and sensible operations between different operators and thus enhances productivity in dragline excavation. In this work, we develop dragline excavation models that can be used for planning and optimizing the dragline operations. The key contribution of this work is to approximate the interaction between the dragline and the terrain with consideration of actual digging and dumping constraints in the 3D environment.

The models that we develop in this work differ from those in [Corke *et al.*, 1997; Luengo *et al.*, 1998; Demirel and Frimpong, 2009], which either capture the kinematics and dynamics of the mechanical components in a dragline or use numerical methods to simulate the interaction between the dragline bucket and the overburden . Our models approximate the dragline-environment interaction for a given dragline position, ignoring oper-

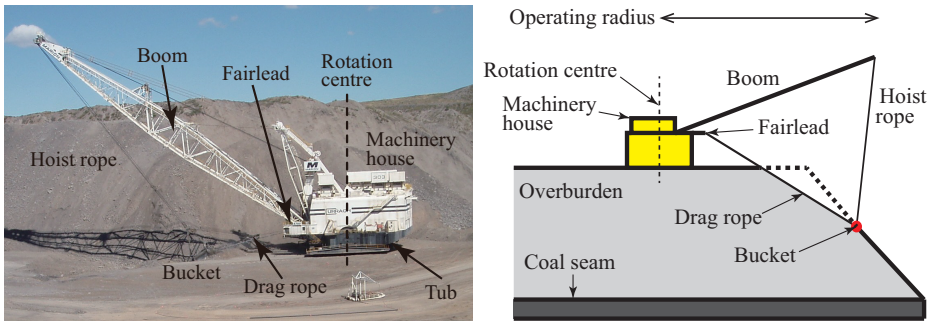

(a) (b)

Figure 1: The dragline excavator. (a) A real dragline (from [Curragh Queensland Mining Limited, 2012] with annotations); (b) Schematic of a dragline.

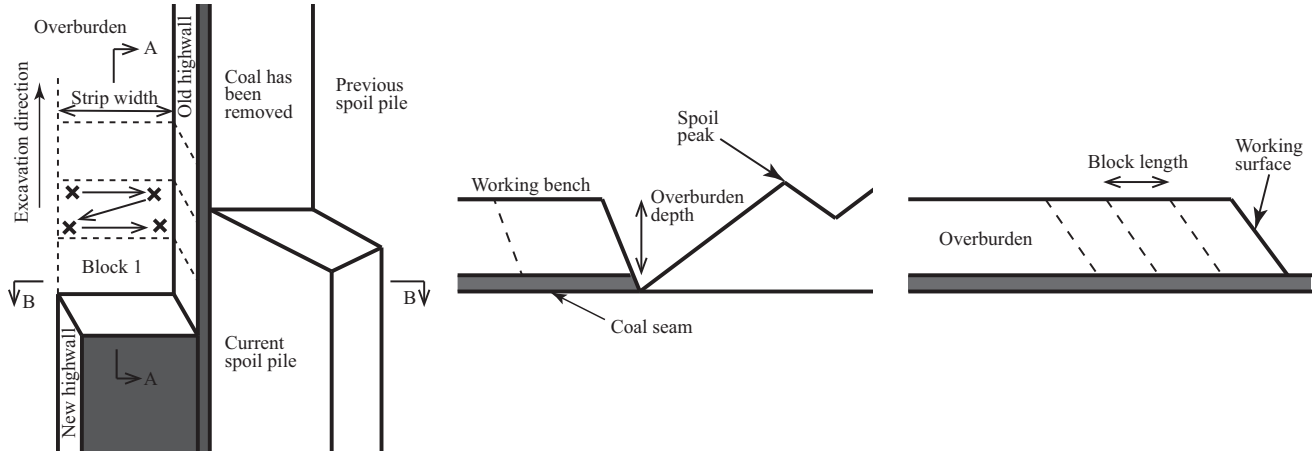

(a) Plan view. (b) Section B-B. (c) Section A-A (Rotated).

Figure 2: Schematic of a mining strip for the dragline. The crosses on the working bench indicate an example dragline positioning sequence through which Block 1 is removed. The material in the block is dug and placed on the adjacent strip by the dragline at these positions, forming and extending the current spoil pile.

ational details at each dig-dump cycle. We consider the bulk movement of material from the block to the spoil pile. We aggregate the digging and dumping actions at each dragline position into a part of the overburden to be removed from the block and the volume of material to be dumped at a sequence of feasible dumping locations over the spoil pile. Combined with the consideration of dragline digging and dumping constraints, we are able to use these models for tactical planning of the dragline operations.

Some dragline excavation models have also been developed for planning and optimization purposes [Sier, 1993; Mirabediny, 1998]. However, they only consider the dragline excavation over 2D sections by splitting the block into sub-blocks and assigning each sub-block to a destination position over the spoil pile. These models fail to capture the geometry of the terrain in the 3D environment during dragline excavation. Dragline excavation planning has been addressed in a 3D environment in [Thornton and Whiten, 2003] using genetic algorithms. However, the resulting terrain profile in the spoil pile does not seem to be realistic and it is unclear how the authors incorporated the digging and dumping constraints in the simulation of the dragline operation.

The dragline working environment in this work is modelled as uniform height grids with cell size of s. The terrain is represented by the heights of the grid points, which we call elements in this work. Each element is represented by its x-y coordinates in the horizontal plane and its vertical height z. Figure 3 shows the height grid representation of a simulated mining strip. We define three areas in the environment: i) the digging area, where the material is removed during the excavation of the block; ii) the dumping area, where the removed ma-

terial is placed; and iii) the working area, where the dragline moves between different positions.

The remainder of this paper is structured as follows: Section 2 presents the formulation of a dragline excavation model with the MILP approach. Section 3 describes the algorithms to approximate the dragline-environment interaction with the geometric approach. Section 4 compares the outputs of these models when computing the digging and dumping limits at a given dragline position. Section 5 discusses the applicability and limitations of the proposed models. Section 6 summarizes the findings in this work and looks at the direction of the future research.

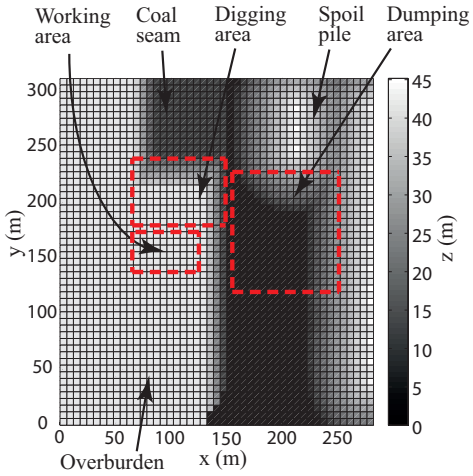

Figure 3: Height grid representation of the environment (plan view). The dragline digging, dumping and working area are indicated by the dashed line boxes while the height level of the terrain is shown in greyscale.

2 MILP Approach

2.1 Mixed-Integer Linear Programming

Mixed-integer linear programming (MILP) is a mathematical programming method that is capable of modelling complex sequencing and scheduling problems with both continuous and discrete decision variables [Bradley *et al.*, 1977]. This feature allows logic propositions to be incorporated into the problem formulation. With customized objective functions, a mixed-integer linear program can produce solutions to the decision variables that optimize an objective function while satisfying the imposed constraints. However, solving a mixed-integer linear program can be computationally expensive due to its incorporation of integer variables. The branch and cut algorithm is the general algorithm to solve this type of problem in modern mathematical solvers, such as Gurobi Optimizer [Gurobi Optimization, 2015].

2.2 Modelling Digging with MILP

At a given dragline position k, the digging action is modelled as the decreased heights of elements inside the digging area. The digging action is denoted by vector $\boldsymbol{u}_k^g = [u_{1k}^g, ..., u_{|\mathcal{S}^g|k}^g]$, where $\mathcal{S}^g$ is the set of indices of elements in the digging area.

At each dragline position, the dragline is only able to dig the material within its operating radius. Furthermore, the rigging between the bucket and the drag rope imposes a minimum distance that the bucket can be from the fairlead. This distance is termed the minimum disengaging radius (MDR). In the 3D environment, the MDR defines a torus in which the material cannot be dug at the current dragline position. The elements that are available for digging under the constraints from the operating radius and the MDR can be determined given the dragline position k and the current initial terrain in the digging area $\boldsymbol{h}_k^{ini,g}$. The indices of these elements are included in set $\mathcal{S}_k^{g,avail}$. An illustration of these two constraints are shown in Figure 4a in a sectional view.

The drag rope interacts with the overburden when the bucket is being dragged along the terrain to collect the material. The drag rope is constrained not to bend over the crests of the terrain in order to minimize its abrasion and extend its service life. This constraint can only be satisfied if the connection between the dug elements (whose heights are reduced at the current dragline position) and the fairlead is not be obstructed by the remaining material in the block. An example of violation of this constraint is shown in Figure 4b. To consider this constraint for element i, we define a set of 'preceding' elements that are affected if the height of element i is decreased, denoted by $\mathcal{S}_{ik}^{g,prece}$. An element is selected to be included in $\mathcal{S}_{ik}^{g,prece}$ if it is within half of the bucket width from the vertical plane that passes through the fairlead and element i, or if it is the closest element to this plane in a row of height grid points in the digging area. Figure 4c illustrates the idea.

Finally, a target terrain is defined in the digging area to avoid accidental removal of the coal seam. The target height of element i is denoted by $H_i^{g,target}$, where $i \in \mathcal{S}^g$.

In MILP, the digging constraints at a dragline position k discussed above are formulated as

$$u_{ik}^g \leq M\alpha_{ik}^{g,chg}, \tag{1}$$

$$\frac{H_k^f - (h_{ik}^{g,ini} - u_{ik}^g)}{D_{ik}^f} - \frac{H_k^f - (h_{i'k}^{g,ini} - u_{i'k}^g)}{D_{i'k}^f} \leq M(1 - \alpha_{ik}^{g,chg}), \tag{2}$$

$$h_{i,k}^{g,ini} - u_{ik}^g \geq H_i^{g,target}, \tag{3}$$

where $i \in \mathcal{S}_k^{g,avail}$, $i' \in \mathcal{S}_{ik}^{g,prece}$, $\alpha_{ik}^{g,chg} = \{0, 1\}$. M is a sufficiently large positive constant. H^f is the height of

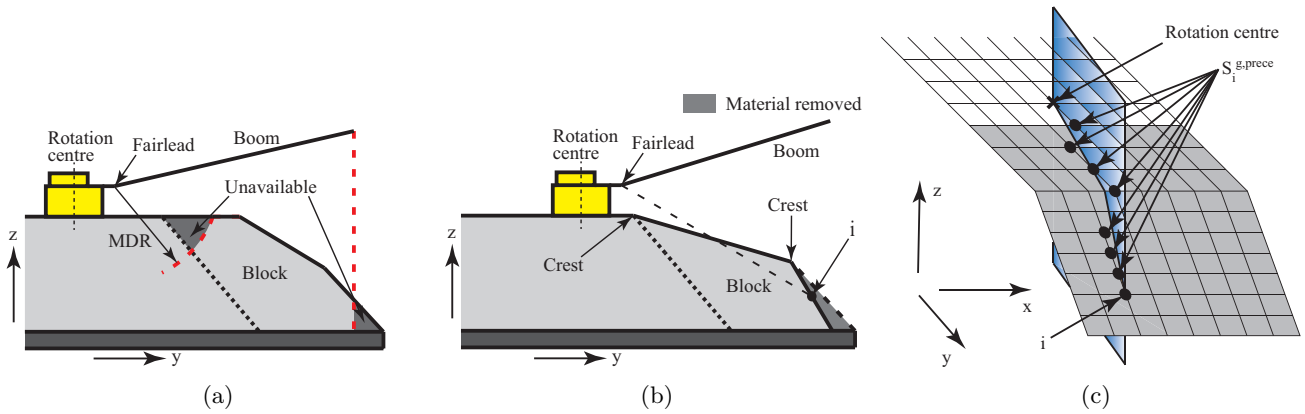

Figure 4: Illustrations of the constraints in dragline digging. (a) Material available for digging under constraints from the operating radius and the MDR; (b) Violation of constraint from drag rope bending in element i when removing the shown material; (c) Preceding elements of element i. The area in gray indicates the digging area.

the fairlead at position k. D^f_{ik} is the horizontal distance from the fairlead to element i at position k. Eq 1 locates elements in the digging area whose heights are reduced during digging at the current dragline position. If the height of element i is reduced, then $\alpha^{g,chg}_{ik} = 1$; otherwise $\alpha^{g,chg}_{ik} = 0$. Eq 2 guarantees that element i can only be dug if it can be reached by a straight and taut drag rope without obstruction of the material at its preceding elements. Eq 3 ensures that the decreased height of i does not exceed its maximum allowable value.

2.3 Modelling Dumping with MILP

Standard draglines dump the material under the tip of the boom, as shown in Figure 5. For a given dragline position k, we define a sequence of N^p_k feasible dumping locations (not necessarily the grid points) along the arc determined by the operating radius. Each of these locations is represented by its x-y coordinates on the horizontal plane. The angular distance between two adjacent dumping locations is fixed and set to 10° in this work. The dumping action is modelled as the volumes of material dumped at these locations and denoted by vector $\boldsymbol{v}^p_k = [v^p_{1k}, ..., v^p_{N^p_k k}]$. A new terrain profile of the spoil pile is formed after dumping. This profile change is captured by the increased heights of the elements in the dumping area denoted by vector $\boldsymbol{u}^p_k = [\boldsymbol{u}^p_{1k}, ..., \boldsymbol{u}^p_{|\mathcal{S}^p|k}]$, where $\mathcal{S}^p$ is the set of indices of elements in the dumping area. The increased height of element i in $\mathcal{S}^p$ is represented by another vector $\boldsymbol{u}^p_{ik} = [u^p_{i1k}, ...u^p_{iN^p_k k}]$ that specifies the increased height of i after dumping at each dumping location.

The terrain change in the dumping area depends primarily on the order of dumping to the defined dumping locations and the volume of material dumped at each location. In this paper, we assume that the dragline dumps the material to the dumping locations in the ascending order of the swing angle, reaching the dumping limit of each dumping location in turn. The swing angle is the angle that the dragline boom passes through when swinging the bucket from the block to the spoil pile and the dumping limit of a dumping location refers to the maximum volume of material that can be dumped at that location without violating the dumping constraints. It should be noted that the modelling of the dumping constraints in this work can be easily modified to comply with a different dumping strategy.

To consider the material settling after dumping, we assume that the new terrain is formed at the angle of repose ϕ^r. The angle of repose is the steepest angle that the surface of a pile of material can make with the horizontal plane [Mehta and Barker, 1994]. Further, the material flow after dumping should be contained within the dumping area in order to comply with the mining plan as well as to avoid covering the coal seam. For this purpose, a 'spoil shell' $\boldsymbol{H}^{p,max}$ is usually defined which specifies the maximum heights of the elements in S^p. The dumping constraints at dragline position k are formulated in MILP as follows

$$u^p_{imk} \leq M\alpha^{p,chg}_{imk}, \tag{4}$$

$$\frac{h^{p,after}_{mk} - (h^{p,ini}_{ik} + \sum_{m'=1}^{m} u^p_{im'k})}{D^p_{imk}} \leq tan(\phi^r), \tag{5}$$

$$\frac{h^{p,after}_{mk} - (h^{p,ini}_{ik} + \sum_{m'=1}^{m} u^p_{im'k})}{D^p_{imk}} \geq \alpha^{p,chg}_{imk} tan(\phi^r) - (1 - \alpha^{p,chg}_{imk}) tan(\phi^r), \tag{6}$$

$$h^{p,ini}_{ik} + \sum_{m=1}^{N^p_k} u^p_{imk} \leq H^{p,max}_i, \tag{7}$$

$$u^p_{ik} = \sum_{m=1}^{N^p_k} u^p_{imk}, \tag{8}$$

$$v^p_{mk} = s \sum_{\forall i \in \mathcal{S}^p} u^p_{imk}, \tag{9}$$

where $i \in \mathcal{S}^p$, $m \in \{1, 2, ..., N^p_k\}$ and $\alpha^{p,chg}_{imk} \in \{0, 1\}$. D^p_{imk} is the horizontal distance between element i and the mth dumping location and $h^{p,after}_{mk}$ is the height of the projected point of the dumping location on the spoil pile after dumping at this location. Here the indices from 1 to N^p_k have been sorted in the ascending order of the swing angle. Eq 4 is used to locate the elements whose heights have increased during dumping at the mth dumping location. If the height of element i has increased, then $\alpha^{p,chg}_{imk} = 1$; otherwise $\alpha^{p,chg}_{imk} = 0$. Eq 5 and 6 constrain the slope between the projected point of the dumping location on the spoil pile and the elements in the dumping area. For elements whose heights have increased, the slope equals to $tan(\phi^r)$, indicating the material flow and settlement. For the remaining elements in the dumping area, the slope is within $[-tan(\phi^r), tan(\phi^r)]$ since $tan(\phi^r)$ is the maximum slope between any two points on the spoil pile profile. Eq 7 specifies the maximum heights of the elements in the dumping area. Eq 8 relates the increased height of an element after dumping at a certain location to its total increased height after dumping at the current dragline position. Eq 9, on the other hand, relates the increased height of an element after dumping at a certain location to the dumping volume at this location.

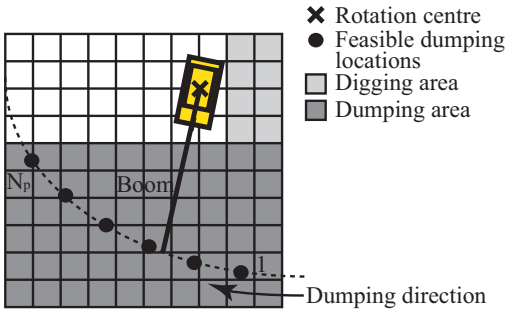

Figure 5: Feasible dumping locations at a dragline position and the dumping direction.

3 Geometric Approach

When planning and optimizing the dragline operations in excavation, it is essential to know the maximum volume of material that can be removed from the block $V^{g,max}_k$ or can be dumped onto the spoil pile $V^{p,max}_k$ with the specified dumping strategy for a given dragline position k. It is straightforward to compute $V^{g,max}_k$ (or $V^{p,max}_k$) by maximizing $\sum u^g_{ik}$ (or $\sum v^p_{mk}$) subject to the mixed-integer digging (or dumping) constraints formulated in the previous section. However, solving a MILP can be slow, even with the state of art commercial solvers. Therefore, we propose two geometric algorithms, GeomMaxDig and GeomMaxDump, to approximate the solutions of solving the MILPs when computing $V^{g,max}_k$ and $V^{p,max}_k$.

3.1 GeomMaxDig

The algorithm for approximating the results of maximizing the digging volume by MILP is outlined in Algorithm 1. For a given element $i \in \mathcal{S}^{g,avail}_k$, if any elements in $\mathcal{S}^{g,precе}_{ik}$ are within the MDR, then $u^{g,max}_{ik}$ is computed based on the minimum gradient between the fairlead and the preceding elements within the MDR. Otherwise, $u^{g,max}_{ik}$ is computed based on the gradient between the fairlead and the preceding element closest to the fairlead. However, the drag rope bending constraint may still be violated between element i and its preceding elements outside the MDR. Therefore, we iteratively apply another algorithm, HeightFix, to check the gradient between the fairlead and the preceding elements of i after the previously computed digging action and correct the decreased height of i if the drag rope bending constraint is violated. HeightFix is outlined in Algorithm 2.

3.2 GeomMaxDump

The algorithm for approximating the results of maximizing the dumping volume by MILP is outlined in Algorithm 3. For each dumping location, we first compute the maximum height of its projected point on the spoil pile by interpolating the heights of the neighbouring elements in the spoil shell. Then we assume the slope between this point and each element in the dumping area equals to the angle of repose and compute the heights of the elements after dumping. For a particular element, if this computed height is larger than its initial height before dumping, then the maximum increased height of this element equals the difference between these two values. Otherwise the height of this element remains the same.

4 Simulation Results

We create a simulated dragline working environment with representative parameters shown in Table 1. Figures 6 and 7 compare the change of terrain in the digging and dumping area from the initial terrain when we maximize the digging and dumping volume using the MILP and geometric methods at the same dragline positions. For visualization, we highlight the terrain in the digging and dumping area, respectively. The value of *max_iter* we choose for Algorithm 1 is 2.

Input : Dragline position k; Initial terrain in the digging area $\boldsymbol{h}_k^{g,ini}$ and maximum number of iterations *max_iter* in HeightFix
Output: Maximum volume of material that can be removed $V_k^{g,max}$ and digging action $\boldsymbol{u}_k^{g,max}$

begin
  foreach $i \in \mathcal{S}_k^{g,avail}$ **do**
    $g_1^{min} \leftarrow 999$;
    $flag \leftarrow 0$;
    $D^{f,min} \leftarrow 999$;
    $g_2^{min} \leftarrow 999$;
    foreach $j \in \mathcal{S}_{ik}^{g,prece}$ **do**
      if *element j is within the MDR* **then**
        $flag \leftarrow 1$;
        $g^{prece,mdr} = \frac{H_k^f - (h_{jk}^{g,ini} - u_{jk}^g)}{D_{jk}^f}$;
        if $g^{prece,mdr} < g_1^{min}$ **then**
          $g_1^{min} \leftarrow g^{prece,mdr}$;
        end
      end
      if $D_{jk}^f < D^{f,min}$ *and* $flag == 0$ **then**
        $D^{f,min} \leftarrow D_{jk}^f$;
        $g_2^{min} \leftarrow \frac{H_k^f - (h_{jk}^{g,ini} - u_{jk}^g)}{D_{jk}^f}$;
      end
    end
    if $flag == 1$ **then**
      $u_{ik}^{g,max} = h_{ik}^{g,ini} - (H_k^f - g_1^{min} D_{ik}^f)$;
    else
      $u_{ik}^{g,max} = h_{ik}^{g,ini} - (H_k^f - g_2^{min} D_{ik}^f)$;
    end
  end
  for $i = 1$ **to** *max_iter* **do**
    $\boldsymbol{u}_k^{g,max} \leftarrow$ `HeightFix(`$\boldsymbol{h}_k^{g,ini}, \boldsymbol{u}_k^{g,max}$`)`;
  end
  $V_k^{g,max} = \sum_{\forall i \in \mathcal{S}^g} u_{ik}^{g,max}$;
end

Algorithm 1: GeomMaxDig

Input : Dragline position k; Initial terrain in the digging area $\boldsymbol{h}_k^{g,ini}$
Output: Digging action $\boldsymbol{u}_k^{g,max}$

begin
  foreach $i \in \mathcal{S}_k^{g,avail}$ **do**
    $g^{min,prece} \leftarrow 999$;
    foreach $j \in \mathcal{S}_{ik}^{g,prece}$ **do**
      if *element j is outside the MDR* **then**
        $g^{prece} = \frac{H_k^f - (h_{jk}^{g,ini} - u_{jk}^g)}{D_{jk}^f}$;
        if $g^{prece,mdr} < g^{min,prece}$ **then**
          $g^{min,prece} \leftarrow g^{prece}$;
        end
      end
    end
    if $H_k^f - g^{min,prece} D_{ik}^f < u_{ik}^{g,max}$ **then**
      $u_{ik}^{g,max} = h_{ik}^{g,ini} - (H_k^f - g^{min,prece} D_{ik}^f)$;
    end
  end
end

Algorithm 2: HeightFix

From Figure 6 and 7, it can be seen that the volume of material removed from the block or dumped onto the spoil pile obtained using the geometric method is almost identical to the one obtained from solving the MILPs. Further, the terrain change in the digging or dumping area is very similar.

5 Discussion

The dragline operation planning is a sequential decision making problem, where the aim is to compute the sequence of positioning, digging and dumping actions that optimizes a given objective (e.g., operation time). The mixed-integer linear program formulated in this work is able to produce the digging and dumping actions that optimize any customized objective functions. However, the optimization is based on a given sequence of dragline positions. One may formulate another mathematical model with MILP that incorporates the planning of dragline positions. But it is not possible to obtain the solution within a reasonable computation time given the unknown number of dragline positions and an additional huge number of binary variables included.

The potential of using the geometric method is illustrated in Table 2 where we compare the performance of the MILP and geometric methods in maximizing the digging and dumping volume at 50 different dragline positions given the same initial terrain in the digging and dumping area. With similar results in the digging and dumping actions, the geometric method requires significantly less computation time than the MILP method. Therefore, it is tractable to apply simulation-based optimization methods (e.g., approximate dynamic programming [Powell, 2007], heuristic search [Hart *et al.*, 1968]) with the geometric model to address the dragline operation planning problem. However, currently the geometric model is only able to simulate the terrain change when maximizing the digging and dumping volume. Proper discretization of the feasible digging and dumping action space is required in order to simulate the excavation process at different dragline positions using the geometric model before it can be used in any simulation-based optimization method.

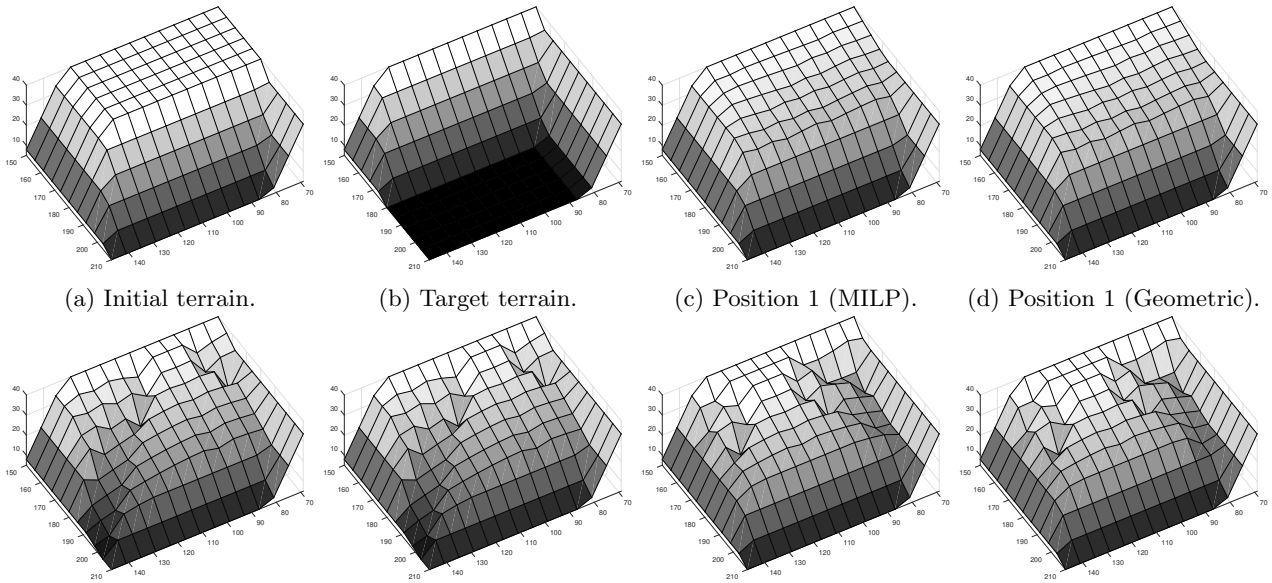

(a) Initial terrain. (b) Target terrain. (c) Position 1 (MILP). (d) Position 1 (Geometric).

(e) Position 2 (MILP). (f) Position 2 (Geometric). (g) Position 3 (MILP). (h) Position 3 (Geometric).

Figure 6: Maximizing the volume of material removed from the block with the MILP and the geometric methods for 3 positions for the same initial terrain in the digging area shown in (a). The size of each cell is $6m \times 6m$.

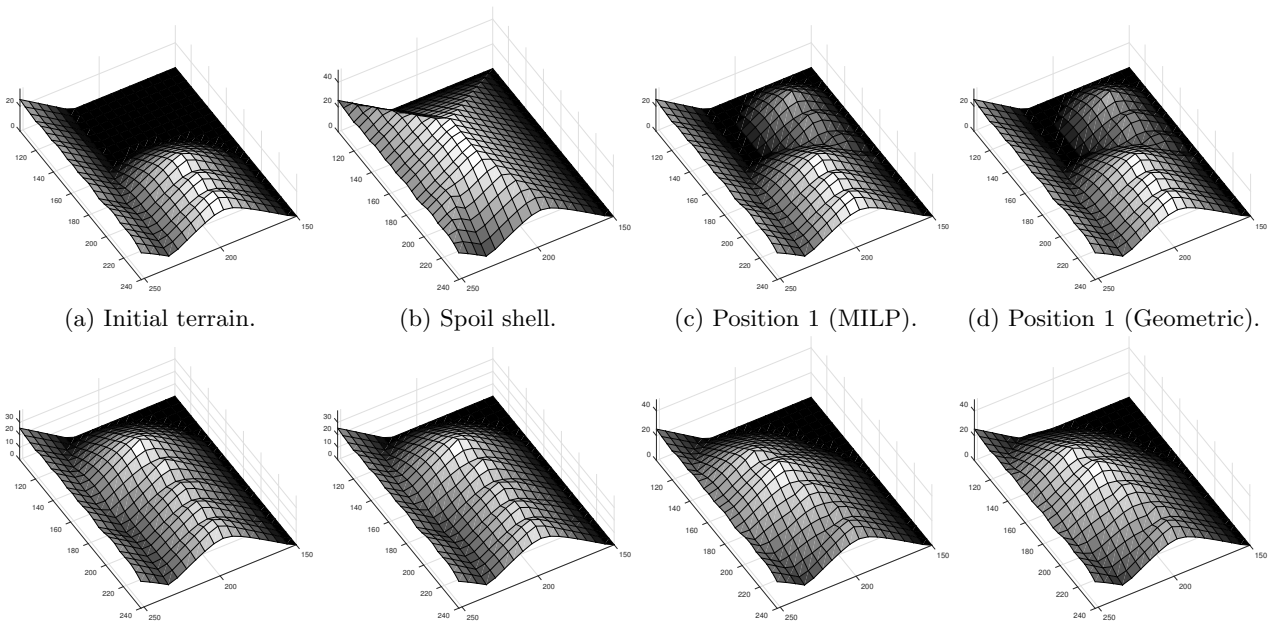

(a) Initial terrain. (b) Spoil shell. (c) Position 1 (MILP). (d) Position 1 (Geometric).

(e) Position 2 (MILP). (f) Position 2 (Geometric). (g) Position 3 (MILP). (h) Position 3 (Geometric).

Figure 7: Maximizing the volume of material dumped onto the spoil pile with the MILP and the geometric methods for 3 positions for the same initial terrain in the dumping area shown in (a). The size of each cell is $6m \times 6m$.

Input : Dragline position k; Initial terrain in the dumping area $\boldsymbol{h}_k^{p,ini}$; Spoil shell $\boldsymbol{H}^{p,max}$
Output: Maximum volume of material that can be dumped $V^{p,max}$ and dumping action $\boldsymbol{v}_k^{p,max}$

begin
  $\boldsymbol{h}_k^{p,ini,temp} \leftarrow \boldsymbol{h}_k^{p,ini}$, $\boldsymbol{u}_k^{p,max} \leftarrow \boldsymbol{0}$;
  `// increasing swing angle with` m
  for $m \leftarrow 1$ **to** N_k^p **do**
    $h_{mk}^{p,after} \leftarrow$ `InterpHMax(`m,$\boldsymbol{H}^{p,max}$`)`;
    foreach $i \in \mathcal{S}^p$ **do**
      $h_{ik}^{p,temp} \leftarrow h_{mk}^{p,after} - \tan(\phi^r) D_{imk}^p$;
      if $h_{ik}^{p,temp} > h_{ik}^{p,ini,temp}$ **then**
        $u_{imk}^{p,max} = h_{ik}^{p,temp} - h_{ik}^{p,ini,temp}$;
      else
        $u_{imk}^{p,max} = 0$;
      end
      $h_{ik}^{p,ini,temp} \leftarrow h_{ik}^{p,ini,temp} + u_{imk}^{p,max}$;
      $u_{ik}^{p,max} \leftarrow u_{ik}^{p,max} + u_{imk}^{p,max}$;
    end
    $v_{mk}^{p,max} = \sum_{\forall i \in \mathcal{S}^p} u_{imk}^{p,max}$;
  end
  $V^{p,max} = \sum_{\forall m \in N_k^p} v_{mk}^{p,max}$;
end

Algorithm 3: GeomMaxDump

6 Conclusions and Future Work

In this paper, we propose two methods to approximate the interaction between the dragline and the environment during dragline excavation. Both of these methods can be used to determine the maximum volume of material that can be removed from the block or dumped onto the spoil pile for a given dragline position and initial terrain, as well as the corresponding digging and dumping actions. The MILP method provides more flexibility in determining the digging and dumping limits and planning the dragline operations within these limits to achieve a specified optimization objective. However, it may only be tractable for a given positioning sequence. On the other hand, the geometric method is significantly less computationally expensive for simulating the excavation process. Therefore, it is tractable to use simulation-based optimization methods with an improved geometric model to solve the dragline operation planning problem. This will be investigated in future work.

In the future, we also look to validate our models by comparing the results from our models to those obtained from some commercial software, such as 3d-Dig [Earth Technology, 2014]. We will also apply the proposed models to the real strip data to evaluate their abilities to deal with more complex geometry in the actual mining environment.

Table 1: Parameters in simulated environment.

Block length	$30m$
Strip width	$66m$
Overburden depth	$35m$
Coal depth	$5m$
Swell factor	1.25
Angle of repose	$37°$
Digging area	$4680m^2$
Dumping area	$14076m^2$
Operating radius	$111.5m$
Minimum disengaging radius	$15m$

Table 2: Computation time in maximizing the digging and dumping volume with MILP and geometric methods for 50 dragline positions (average). The size of each cell is $6m \times 6m$. The computation was performed on a desktop with a 3.4GHz CPU and 16.0GB RAM and the mathematical programs were solved by Gurobi 6.5.

	MILP	Geometric
Max digging	$3.56s$	$0.045s$
Max dumping	$3.31s$	$0.008s$

Acknowledgement

The first author thanks the School of Mechanical and Mining Engineering at The University of Queensland for offering the Advisor Start-up Research Higher Degree Living Allowance Scholarship to support his research. The authors would also like to thank Professor Ross McAree for introducing this problem and Dr. Michael Forbes for helpful comments during this research.

References

[Bradley *et al.*, 1977] Stephen Bradley, Arnoldo Hax, and Thomas Magnanti. Applied mathematical programming. 1977.

[Corke *et al.*, 1997] Peter I Corke, Graeme J Winstanley, and Jonathan M Roberts. Dragline modelling and control. In *Robotics and Automation, 1997. Proceedings., 1997 IEEE International Conference on Robotics and Automation*, volume 2, pages 1657–1662. IEEE, 1997.

[Corke *et al.*, 2006] Peter Corke, Graeme Winstanley, Matthew Dunbabin, and Jonathan Roberts. Dragline automation: Experimental evaluation through productivity trial. In *Field and Service Robotics*, pages 459–468. Springer, 2006.

[Curragh Queensland Mining Limited, 2012] Curragh Queensland Mining Limited. Curragh dragline. `https://en.wikipedia.org/wiki/File:Curragh_Dragline_3.JPG`, 2012. Accessed: 2015-04-13.

[Demirel and Frimpong, 2009] Nuray Demirel and Samuel Frimpong. Dragline dynamic modelling for efficient excavation. *International Journal of Mining, Reclamation and Environment*, 23(1):4–20, 2009.

[Earth Technology, 2014] Earth Technology. Earth technology software & mathematical modelling. `http://www.3ddig.com/`, 2014. Accessed: 2014-09-30.

[Gurobi Optimization, 2015] Inc. Gurobi Optimization. Gurobi optimizer reference manual, 2015.

[Hart *et al.*, 1968] Peter E Hart, Nils J Nilsson, and Bertram Raphael. A formal basis for the heuristic determination of minimum cost paths. *IEEE transactions on Systems Science and Cybernetics*, 4(2):100–107, 1968.

[Humphrey and Wagner, 2011] James Humphrey and Joshua Wagner. Mechanical excavation, loading, and hauling. In Peter Darling, editor, *SME mining engineering handbook*, volume 1, chapter 10.3, pages 903–929. SME, 2011.

[Luengo *et al.*, 1998] Oscar Luengo, Sanjiv Singh, and Howard Cannon. Modeling and identification of soil-tool interaction in automated excavation. In *Intelligent Robots and Systems, 1998. Proceedings., 1998 IEEE/RSJ International Conference on*, volume 3, pages 1900–1906. IEEE, 1998.

[Mehta and Barker, 1994] Anita Mehta and GC Barker. The dynamics of sand. *Reports on Progress in Physics*, 57(4):383, 1994.

[Mirabediny, 1998] Hamid Mirabediny. *A dragline simulation model for strip mine design and development.* PhD thesis, Department of Civil and Mining Engineering-Faculty of Engineering, University of Wollongong, 1998.

[Powell, 2007] Warren B Powell. *Approximate Dynamic Programming: Solving the curses of dimensionality*, volume 703. John Wiley & Sons, 2007.

[Sier, 1993] D Sier. Optimised dragline planning model. Technical report, 1993.

[Thornton and Whiten, 2003] Darren Thornton and Bill Whiten. Optimization of dragline excavation. Technical report, Julius Kruttschnitt Mineral Research Centre, 2003.